Solid State Communications 281 (2018) 38–43

Contents lists available at ScienceDirect

Solid State Communications

journal homepage: www.elsevier.com/locate/ssc

Communication

Electronic structure, elastic and phonon properties of perovskite-type hydrides $MgXH_3$ (X = Fe, Co) for hydrogen storage

Abdullah Candan[a], Mustafa Kurban[b,*]

[a] Department of Machinery and Metal Technology, Ahi Evran University, 40100, Kırşehir, Turkey
[b] Department of Electronics and Automation, Ahi Evran University, 40100, Kırşehir, Turkey

ARTICLE INFO

Communicated by J.R. Chelikowsky

Keywords:
Perovskite hydrides
Hydrogen storage
Elastic constants
Electronic structure

ABSTRACT

Metal–hydrogen systems have been continuously investigated due to the ability of metallic atoms to absorb large amounts of hydrogen. According to this viewpoint, the electronic structure, elastic and phonon properties of perovskite hydrides $MgXH_3$ (X = Fe, Co) are searched using ab initio calculations based on density-functional theory (DFT) in this study. The lattice constants, bulk modulus, second order elastic modulus, anisotropy factors, Poisson's ratio, Young's and Shear moduli are calculated. From the elastic constants, both hydrides were found to be stable mechanically. According to obtained results, $MgFeH_3$ and $MgCoH_3$ can be classified as brittle and ductile material, respectively. Both hydrides show a metallic character due to very strong electron phonon interaction. The electronic band structures, phonon dispersion curves, the corresponding total and partial density of states (DOS), as well as the specific heat capacity, entropy and phonon free energy in terms of temperature are also researched for the first time in this study.

1. Introduction

Recently, the working principles of hybrid perovskites have received enormous attention for making next-generation solar cells [1,2] because they are considerably efficient at converting light to electricity. The perovskites have desirable electronic structure properties such as bandgap in the visible range and a light absorption efficiency, which are comparable with that of Si or GaAs [3–5] which is the best performing semiconductors.

Moreover, hybrid metal halide perovskites increase considerably the efficiencies from a value of 3.8% to overcome the 20% in a short period of time [6–8]. Beyond their use in solar cells, other considerable features have been displayed in various fields such as sunlight-to-fuel conversion, light emitting devices, sensors photodetectors and lasers [9–13]. For example, the spin–orbit coupling effect in $CH_3NH_3PbI_3$ can change the positions of the minimum of the conduction band and the maximum of the valence band in k space [14]. In addition, the hydride $LiBeH_3$ displays high-temperature superconductivity [15]. $NaMgH_3$ was also pointed out as the excellent hydrogen mobility of the hydride perovskite structure [16].

All the mentioned above examples indicate the role of perovskite hydrides and invite further investigation about the electronic structure and structural properties of perovskite hydrides to obtain desirable properties. Especially, ternary hydrides including Mg and transition metals are very attractive materials for hydrogen and energy storage [17]. At this view point, earlier studies with $MgXH_3$ type perovskite hydride structures have dealt mainly with hydride formation energies for X = Sc, Ti, V, Cr, Mn, Fe, Co, Ni, Cu and Zn 3d transition metals [18]. Moreover, the metal-hydrogen bonding properties, crystal structure and lattice dynamics of the perovskite hydride $MgNaH_3$ were investigated for hydrogen storage [19]. Among the perovskite hydrides, $MgKH_3$, $MgRbH_3$ and $MgCsH_3$ having available crystallographic information were also reported [20–24]. To our knowledge, there is no any information on the electronic structure, elastic, phonon properties as well as the specific heat capacity, entropy and phonon free energy in terms of temperature of the perovskite hydrides $MgXH_3$ (X = Fe, Co) in the literature. Thus, the major aim of this study is to probe the features mentioned above of the perovskite hydrides $MgXH_3$ (X = Fe, Co) compounds using density functional theory (DFT) approach.

2. Computational details

The electronic structure, elastic and phonon properties of perovskite hydrides $MgXH_3$ (X = Fe, Co) have been investigated using DFT implemented in VASP code [25] in MedeA program [26]. For pseudopotentials of the perovskite hydrides, the electronic exchange correlation potential was performed within the generalized gradient approximation (GGA) [27] in the scheme of Perdew-Burke-Ernzerhof (PBE) [28].

* Corresponding author.
E-mail addresses: mkurbanphys@gmail.com, mkurban@ahievran.edu.tr (M. Kurban).

https://doi.org/10.1016/j.ssc.2018.07.004
Received 14 April 2018; Received in revised form 25 June 2018; Accepted 2 July 2018
Available online 03 July 2018
0038-1098/

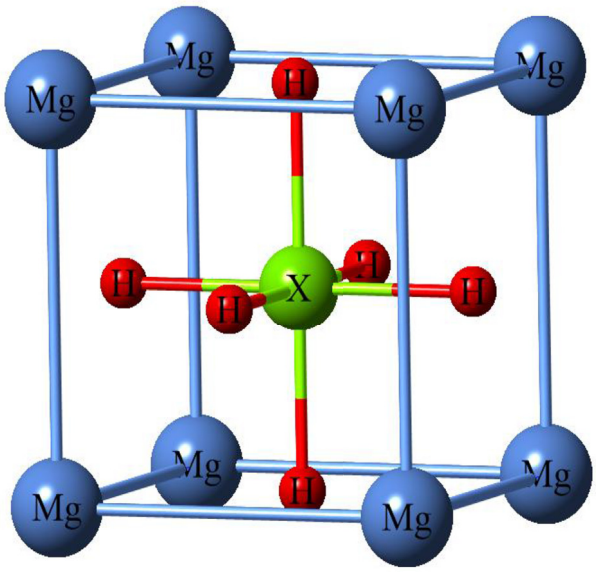

Fig. 1. Crystal structure of the cubic perovskite hydrides $MgXH_3$ (X = Fe, Co).

Generating pseudopotentials, the distribution of electrons is taken as Mg ($2p^6 3s^2$), Fe ($3p^6 4s^2 3d^6$) and Co ($3p^6 4s^2 3d^7$). An energy cut-off 327 eV was found to be adequate for the calculation. The Brillouin zone integration was implemented on a Monkhorst-Pack [4] 6 × 6 × 6 k-point mesh with a Methfessel–Paxton [29] smearing of 0.225 eV for $MgFeH_3$ and $MgCoH_3$. The elastic constants were predicted using the stress-finite strain technique. The phonon dispersion curves of the perovskite hydrides have been calculated [30] using the Hellmann–-Feynman (HF) theorem. The lattice constants are obtained with the process of geometrical optimization. The lattice constant values are used in other calculations.

3. Results and discussion

3.1. Structural properties

Perovskite hydrides $MgXH_3$ (X = Fe, Co) belong to the Pm-3m (No: 221) space group. The unit cell of the perovskite compounds are found using the fractional coordinates for Mg atom; in the corner (0, 0, 0), for an X transitional metal atom in the center; (0.5, 0.5, 0.5) and for three H atoms in octahedral sites at the face centers; (0.5, 0.5, 0), (0.5, 0, 0.5) and (0, 0.5, 0.5), respectively [31]. Crystal structure of the cubic $MgXH_3$ (X = Fe, Co) compounds are given in Fig. 1. The lattice constants (a_0) and bulk modulus (B) of $MgXH_3$ (X = Fe and Co) compounds are tabulated in Table 1. The lattice constants of $MgFeH_3$ and $MgCoH_3$ compounds are found to be 3.280 and 3.288 Å, respectively. We can conclude that the lattice constants $MgCoH_3$ compound are greater than that of $MgFeH_3$ compound. In addition, the bulk modulus value increases with decreasing lattice constants.

Table 2
Total energies (E_T) and formation energies (ΔH_f) of binary intermetallics and their hydrides.

Material	E_T (kJ/mol.atom)	E_T (eV/mol.atom)	ΔH_f (kJ/mol.H_2)
$MgFeH_3$	−1969.081	−20.41	−70.7
$MgCoH_3$	−1892.924	−19.62	−73.8
MgFe	−930.969	−9.65	–
MgCo	−824.553	−8.55	–
H_2	−237.308	−2.46	–

3.2. Elastic properties

$MgXH_3$ (X = Fe, Co) cubic perovskite compounds have only three independent elastic constants (C_{11}, C_{12} and C_{44}). In the literature, there is no experimental information about the elastic constants of these compounds, thus our results for the cubic phase can provide an insight for future investigations. The values of C_{11} and C_{44} decrease from $MgFeH_3$ to $MgCoH_3$, while the value of C_{12} increase from $MgCoH_3$ to $MgFeH_3$ (see Table 1). The bulk modulus (B), shear modulus (G), bulk modulus to shear modulus (B/G), second order elastic modulus (C11, C12 and C44), Young modulus elastic, anisotropy factors (A) and Poisson's ratios (υ) for $MgXH_3$ (X = Fe, Co) cubic perovskite compounds (E) are given in Table 1. The requirement of a cubic crystal to be mechanically stable, second order elastic constants must satisfy the Born stability criteria [32] given in Equation (1). Taking into considering these stability criteria, it was concluded that $MgXH_3$ (X = Fe, Co) compounds are mechanically stable.

$$C_{11} > 0 \quad C_{44} > 0 \quad C_{11} + 2C_{12} > 0 \quad C_{11} - C_{12} > 0 \tag{1}$$

Moreover, the ratios *(B/G)* of the bulk modules *(B)* to the Shear modules *(G)* of Bulk modules (B) of $MgXH_3$ (X = Fe, Co) compounds, the most commonly used empirical criterion proposed by Pugh [33], are given in Table 1. According to this criteria, if the *B/G* ratio of the material is greater than 1.75, the material exhibits ductile behavior, whereas when the *B/G* ratio is less than 1.75, the material shows brittle behavior. From Table 1, the following results are concluded; The *B/G* ratio of the $MgFeH_3$ compound is less than the critical value of 1.75, indicating that the material is brittle. On the other hand, the B/G ratio of the $MgCoH_3$ compound is higher than the critical value of 1.75, indicating that this material is ductile.

The Young's modulus (E) of a material is used to characterize stiffness, and the larger E value means that the material is harder. The values of the calculated Young's modulus are found to be in order: $E(MgFeH_3) > E(MgCoH_3)$. The value of the Poisson's ratio (ν) is close to 0.1 for covalent materials and 0.25 for ionic materials. Therefore, the ionic character of $MgXH_3$ (X = Fe, Co) compounds can be seen from the Poisson ratios (Table 1). The anisotropy factor (A) is a measure of the degree of elastic anisotropy. If the material is elastically isotropic, the value of the anisotropic factor is different from 1 (one). All of the compounds investigated are found to be anisotropic.

3.3. Spin polarized calculations

We have also performed spin polarized calculations on $MgFeH_3$ and $MgCoH_3$ hydrides, which could be expected to form spin polarized

Table 1
The calculated lattice constants (a_0), magnetic moments (M), bulk modulus (B), shear modulus (G), B/G ratio, elastic constants (C_{11}, C_{12} *ve* C_{44}), Young modulus (E), elastic anisotropy factors (A) and Poisson's ratios (υ) of $MgXH_3$ (X = Fe, Co) compounds.

Compounds	a_0 (Å)	M (μB)	B (GPa)	G (GPa)	B/G	C_{11} (GPa)	C_{12} (GPa)	C_{44} (GPa)	E (GPa)	A	ν
$MgFeH_3$	3.280483	–	131.39	75.86	1.73	278.44	57.86	58.81	190.84	0.53	0.258
Spin	3.302858	1.0008									
$MgCoH_3$	3.288151	–	126.36	66.68	1.90	254.92	62.08	51.89	170.11	0.54	0.276
Spin	3.280325	0.0001									

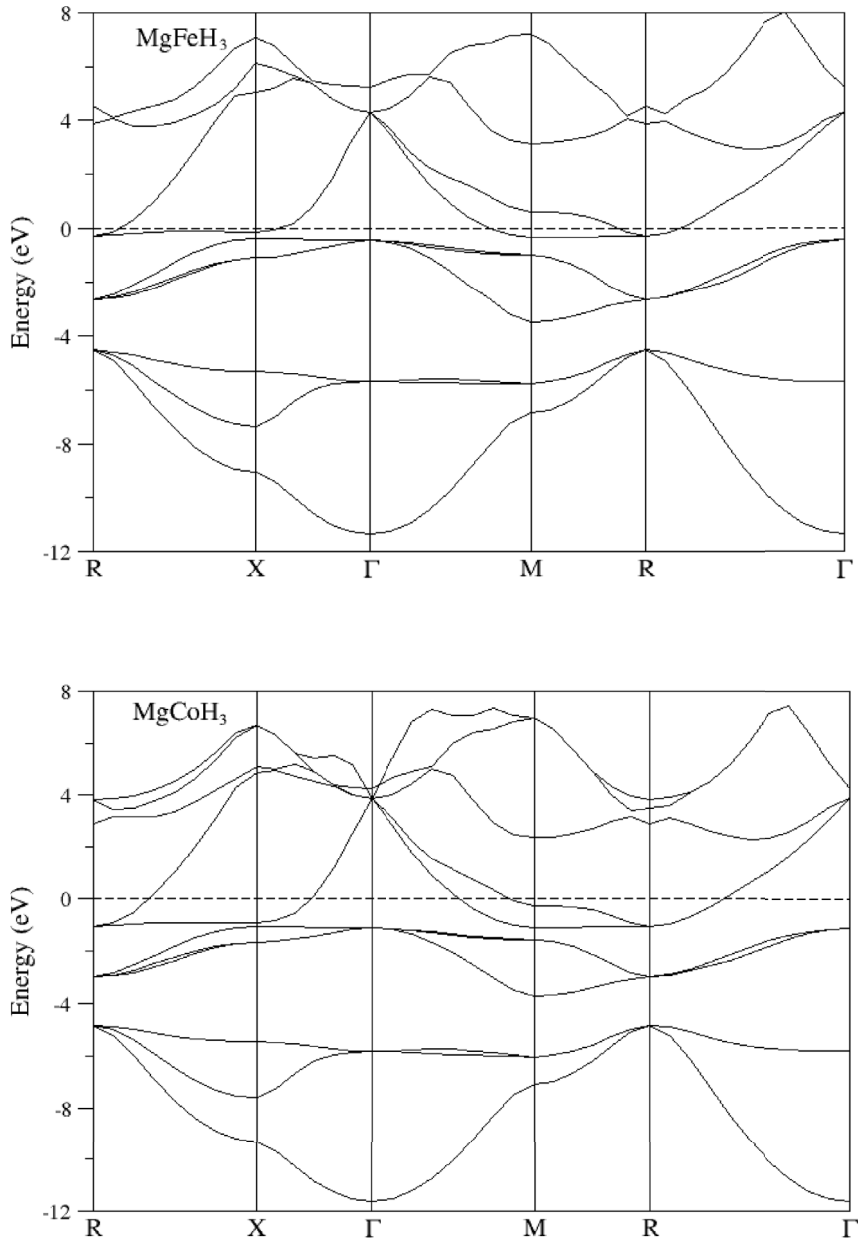

Fig. 2. The electronic band structure for the cubic phase of (a) $MgFeH_3$ and (b) $MgCoH_3$ compounds.

states. When it comes to the limited size of the unit cell, it is not possible directly to investigate anti-ferromagnetic states. Ferromagnetic states are found to be preferred for $MgFeH_3$, and for $MgCoH_3$ only a marginal effect of the spin polarization is seen (Table 1). Moreover, recognizing the ferromagnetic limitations of the unit cell (one transition metal atom), we primarily focus on the unpolarized results. It should, however, be noted the alternate simulations were performed on a larger super cell ($3 \times 3 \times 3$ unit cell), yielding no preferential anti-ferromagnetic states for the hydrides.

3.4. Hydride formation energies

Storage of hydrogen in metal hydrides is possible since many metals react readily with hydrogen forming a stable metal hydride. Formation energies are a significant way to determine if the predicted phased are likely to be stable in this regard. The formation energies given in Table 2 are the energies required to form the hydride phase following the reaction:

$$MgTM + 3/2H_2 \rightarrow MgTMH_3 \quad \text{(where TM is Fe or Co)} \tag{2}$$

The difference of the total energies (E_T) between the hydride phase and sum of H_2 in the gas phase and the energy of MgTM alloy:

$$\Delta H_f(MgTMH_3) = E_T(MgTMH_3) - E_T(MgTM) - 3/2E_T(H_2) \tag{3}$$

The formation energies obtained for $MgFeH_3$ and $MgCoH_3$, $\Delta H_f = -70.7$ and $-73.8 \frac{kJ}{mol}$. H_2, respectively, which indicate the stability of the hydrides. The high stability of $MgFeH_3$ and $MgCoH_3$ can be utilized for hydrogen to be stored in the hydrides.

3.5. Electronic band structure and density of state

The electronic band structure along the high symmetry directions obtained from the calculated equilibrium lattice constants of $MgFeH_3$ and $MgCoH_3$ compounds is demonstrated in Fig. 2. As seen in Fig. 2, there is no forbidden energy gap at the Fermi level for both compounds. In other words, the conduction and valence bands overlap with each other at the Fermi level. Thus, one can conclude that $MgXH_3$ (X = Fe,

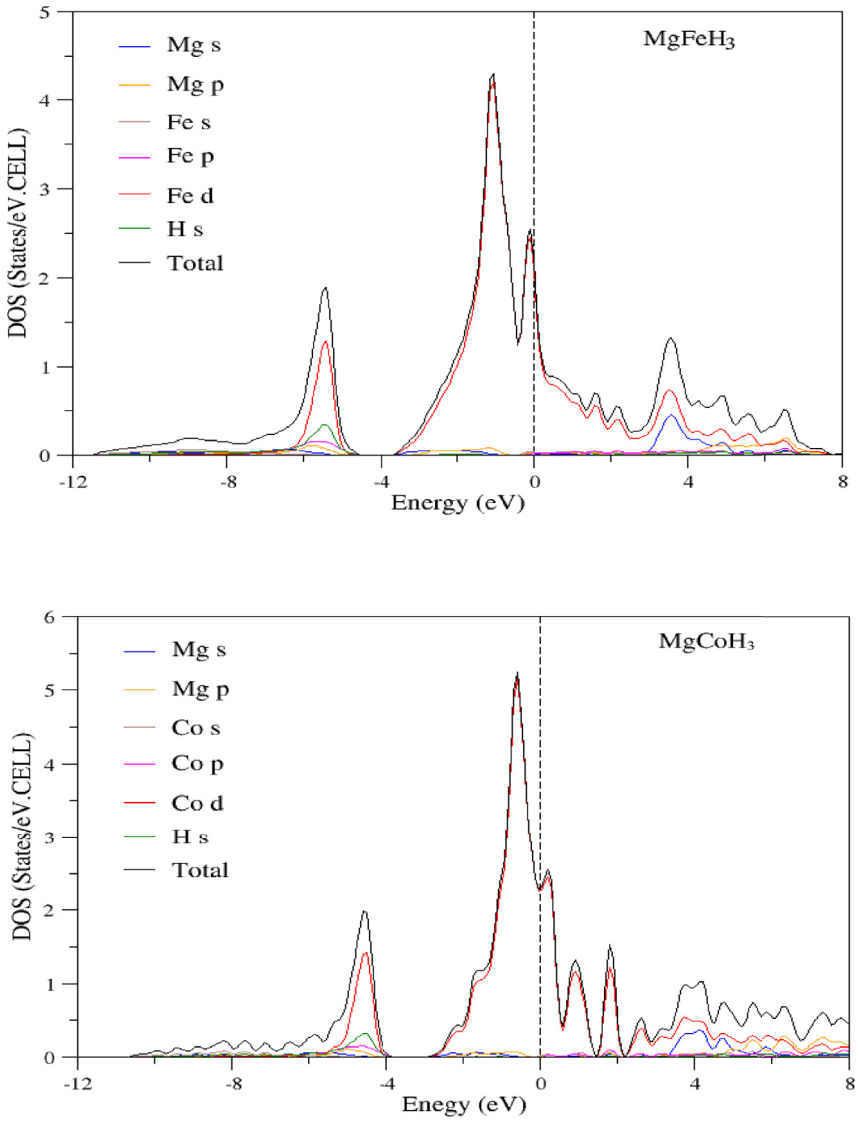

Fig. 3. The partial and total DOS of $MgFeH_3$ and $MgCoH_3$ compounds.

Co) compounds show a metallic character.

For understanding of the electronic contribution, the total and partial density of state curves were also plotted and presented in Fig. 3 for $MgFeH_3$ and $MgCoH_3$ compounds, respectively. From $MgFeH_3$ compound, the sharp peak at about −5.43 eV, below the Fermi level formed by the contribution of the d-orbitals of Fe atom and s-orbitals of H atoms, while the Fermi level formed by the contribution of the d-orbitals of Fe atom. We also find that the valence band is from 0 to 8 eV is mainly due to d-orbitals of Fe atom, s-orbitals of Mg atom and p-orbitals of Mg atom. The valence band is mainly due to the contribution of d-orbitals of Co atom, s- and p-orbitals of Mg atom.

The density of state values at the Fermi level (E_F) were calculated as 2.197 and 2.316 eV for $MgFeH_3$ and $MgCoH_3$, respectively. From the density of state curves (see Fig. 3), it is seen that the conduction band is mainly from the d-orbitals of the Fe and Co atoms and small contributions of s-orbitals of H atoms.

3.6. Phonon properties

In Fig. 4, we plotted the phonon dispersion curves and density of states (DOS) of $MgXH_3$ (X = Fe, Co) compounds along high symmetry directions in the first Brillouin zone. Due to five atoms in the unit cell, there are 15 vibrational phonon modes which are composed of three acoustics and twelve optical modes for any chosen q point. However, the distinct number of branches is reduced along the principal symmetry directions X-Γ and R-Γ because the phonon branches are degenerate in some symmetry directions.

From Fig. 4, there is a gap between the optic-optical phonon modes due to the difference in mass between the atoms Mg, Fe, Co and H atoms. From the total phonon density of state curves (see Fig. 4), this gap is calculated to be 41.12 and 28.53 THz for the $MgFeH_3$ and $MgCOH_3$ compounds, respectively. The calculated zone-center phonon frequencies are found to be 5.72-10.68-13.12-54.19 and 5.27-17.12-18.83-47.48 THz, for the $MgFeH_3$ and $MgCoH_3$ compounds, respectively. The partial density of state curves show that Mg and Fe atoms in the $MgFeH_3$ compound vibrate in the acoustic region while the H atoms vibrate only in the optical region. On the other hand, Mg and Co atoms in the $MgCoH_3$ compound shows vibrations in the acoustic region while only H atoms are vibrated in the optical region.

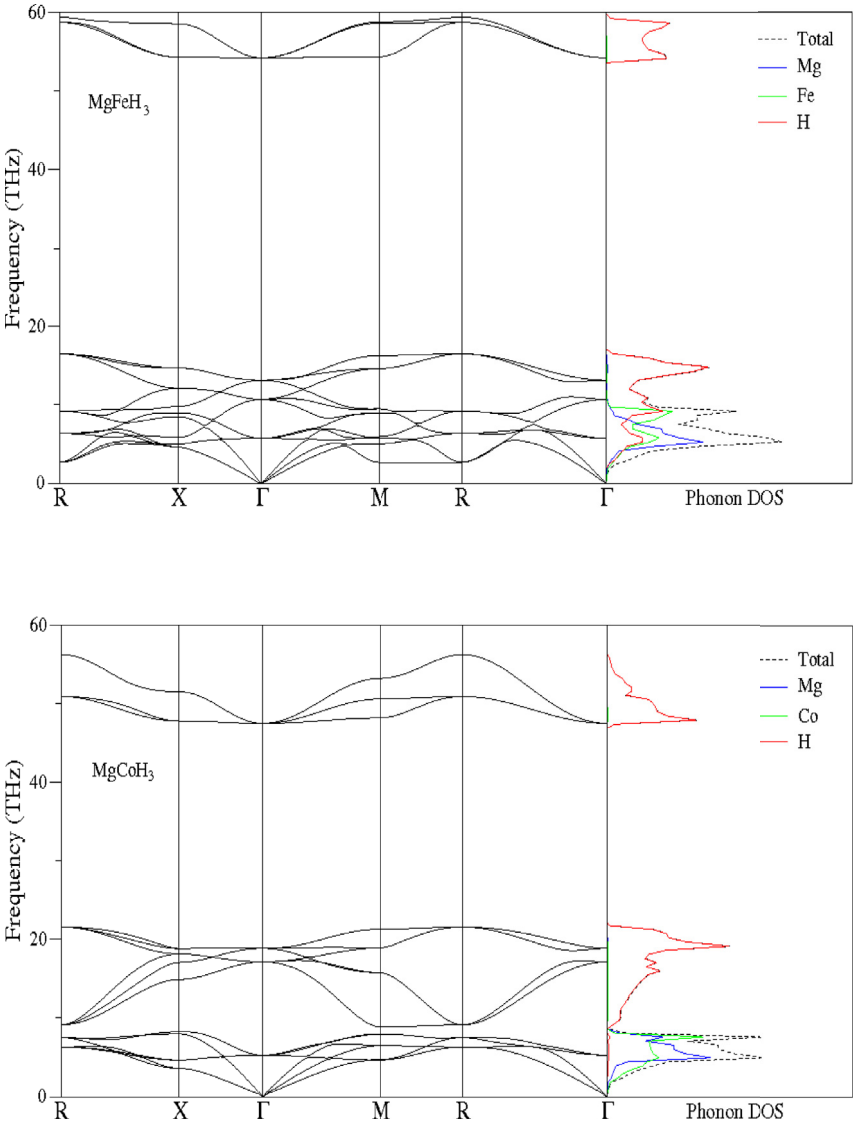

Fig. 4. The phonon dispersion curves and phonon DOS for $MgFeH_3$ and $MgCoH_3$ compounds.

3.7. Thermal properties

The calculated specific heat (C_v) of $MgXH_3$ (X = Fe, Co) compounds as based on temperature is given in Fig. 5 (a). We find a rapid rise in C_v up to about 500 K, then C_v becomes constant at high temperatures, that is, follows the Dulong–Petit's law. As depending on the increase in temperature, C_v of $MgFeH_3$ is sharper than that of $MgCoH_3$ at low temperature region, however; there is no significant differences at high temperature. Moreover, the behavior of the entropy (S) and free energy of $MgXH_3$ (X = Fe, Co) compounds are investigated in term of temperature as shown in Fig. 5 (b) and (c). S increases with the increase in temperature while free energy decreases. The variation of S for $MgFeH_3$ compound is greater than that of $MgCoH_3$.

4. Conclusions

The electronic structure, elastic and phonon properties of perovskite hydrides $MgXH_3$ (X = Fe, Co) have been investigated using DFT approach. The lattice constants (a_0), Bulk modulus (B), shear modulus (G), bulk modulus to shear modulus (B/G), second order elastic modulus (C_{11}, C_{12}, C_{44}) Young modulus (E) elastic, anisotropy factors (A) and Poisson's ratios (v) are searched for the first time in this study. The obtained elastic constants satisfy the mechanical stability criteria. From the B/G ratio, $MgFeH_3$ and $MgCoH_3$ are found to be brittle and ductile, respectively. $MgFeH_3$ and $MgCoH_3$ are found to be anisotropic in nature. The band structure and densities of states show that both hydrides show metallic character which means there is very strong electron phonon interaction. Based on the hydride formation energies, the high stability of $MgFeH_3$ and $MgCoH_3$ can be utilized for hydrogen to be stored in the hydrides. In addition, the phonon frequencies along high symmetry directions indicate that all compounds are mechanically stable without any imaginary phonon frequencies. The heat capacity and entropy increase with the increase in temperature, but free energy decreases.

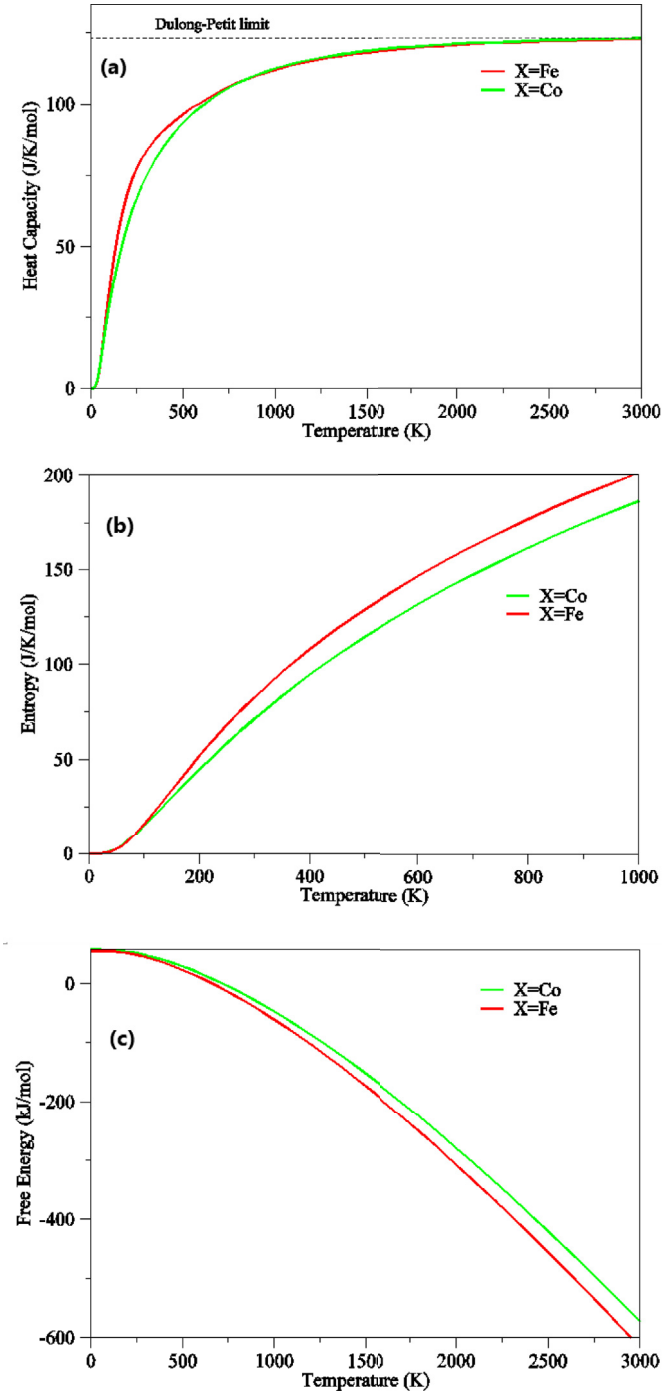

Fig. 5. (a) The specific heats at constant volume, (b) entropy (S) and (c) phonon free energy versus temperature for $MgFeH_3$ and $MgCoH_3$ compounds.

References

[1] M.A. Green, A. Ho-Baillie, H.J. Snaith, Nat. Photon. 8 (2014) 506.
[2] H.J. Snaith, J. Phys. Chem. Lett. 4 (2013) 3623.
[3] C. Motta, F. El-Mellouhi, S. Kais, N. Tabet, F. Alharbi, S. Sanvito, Nat. Commun. 6 (2015) 7026.
[4] T. Wang, B. Daiber, J.M. Frost, S.A. Mann, E.C. Garnett, A. Walsh, B. Ehrler, Energy Environ. Sci. 10 (2017) 509.
[5] E.M. Hutter, M.C. Gélvez-Rueda, A. Osherov, V. Bulovič, F.C. Grozema, S.D. Stranks, T.J. Savenije, Nat. Mater. 16 (2017) 115.
[6] A. Kojima, K. Teshima, Y. Shirai, T. Miyasaka, J. Am. Chem. Soc. 131 (2009) 6050.
[7] H. Zhou, Q. Chen, G. Li, S. Luo, T.-b. Song, H.-S. Duan, Z. Hong, J. You, Y. Liu, Y. Yang, Science 345 (2014) 542.
[8] N.J. Jeon, J.H. Noh, W.S. Yang, Y.C. Kim, S. Ryu, J. Seo, S.I. Seok, Nature 517 (2015) 476.
[9] J. Luo, J.-H. Im, M.T. Mayer, M. Schreier, M.K. Nazeeruddin, N.-G. Park, S.D. Tilley, H.J. Fan, M. Gratzel, Science 345 (2014) 1593.
[10] C. Muthu, S.R. Nagamma, V.C. Nair, RSC Adv. 4 (2014) 55908.
[11] Y. Fang, Q. Dong, Y. Shao, Y. Yuanand, J. Huang, Nat. Photon. 9 (2015) 679.
[12] Z.-K. Tan, R.S. Moghaddam, M.L. Lai, P. Docampo, R. Higler, F. Deschler, M. Price, A. Sadhanala, L.M. Pazos, D. Credgington, F. Hanusch, T. Bein, H.J. Snaith, R.H. Friend, Nat. Nanotechnol. 9 (2014) 687.
[13] G. Xing, N. Mathews, S.S. Lim, N. Yantara, X. Liu, D. Sabba, M. Grötzel, S. Mhaisalkar, T.C. Sum, Nat. Mater. 13 (2014) 476.
[14] F. Zheng, L.Z. Tan, S. Liu, A.M. Rappe, Nano Lett. 15 (2015) 7794.
[15] A.W. Overhauser, Phys. Rev. B 35 (1987) 411.
[16] D. Pottmaier, E.R. Pinatel, J.G. Vitillo, S. Garroni, M. Orlova, M.D. Baro, et al., Chem. Mater. 23 (2011) 2317.
[17] L. Mendoza-Zélis, M. Meyer, L. Baum, Int. J. Hydrogen Energy 36 (2011) 600.
[18] T. Vegge, L.S. Hedegaard-Jensena, J. Bondea, T.R. Muntera, J.K. Nørskova, J. Alloy. Comp. 386 (2005) 1.
[19] H. Wu, W. Zhou, T.J. Udovic, J.J. Rush, T. Yildirim, Chem. Mater. 20 (2008) 2335.
[20] A. Bouamrane, J.P. Laval, J.-P. Soulie, J.P. Bastide, Mater. Res. Bull. 35 (2000) 545.
[21] H.-H. Park, M. Pezat, B. Darriet, P. Hagenmuller, Rev. Chim. Miner. 24 (1987) 525.
[22] A.J. Maeland, W.D.Z. Lahar, Phys. Chem. 179 (1993) 181.
[23] F. Gingl, T. Vogt, E. Akiba, K. Yvon, J. Alloy. Comp. 125 (1999) 282.
[24] B. Bertheville, P. Fischer, K. Yvon, J. Alloy. Comp. 151 (2002) 330.
[25] G. Kresse, J. Hafner, Phys. Rev. B 47 (1993) 558.
[26] G. Kresse, J. Furthmuller, Phys. Rev. B 54 (1993) 1169.
[27] J.P. Perdew, K. Burke, M. Ernzerhof, Phys. Rev. Lett. 77 (1996) 3865.
[28] H.J. Monkhorst, J.D. Pack, Phys. Rev. B 13 (1976) 5188.
[29] M. Methfessel, A.T. Paxton, Phys. Rev. B 40 (1989) 3616.
[30] K. Parlinski, Z.Q. Li, Y. Kawazoe, Phys. Rev. Lett. 78 (1997) 4063.
[31] K. Kishida, K. Goto, H. Inui, Acta Crystallogr. Sect. B Struct. Sci. 65 (2009) 405.
[32] M. Born, K. Huang, Dynamical Theory of Crystal Lattices, Oxford University Press, Oxford, 1954.
[33] S.F. Pugh, Philos. Mag. 45 (1954) 823.